

Upper extremity augmentation of lower extremity kinetics during countermovement vertical jumps

MICHAEL E. FELTNER,* DANIEL J. FRASCHETTI and ROBERT J. CRISP

Department of Sports Medicine and Physical Education, Pepperdine University, Malibu, CA 90263, USA

Accepted 26 July 1998

Twenty-five volleyball players (14 males, 11 females) were videotaped (60 Hz) performing countermovement vertical jumps with and without an arm swing. Ground reaction force and video-based coordinate data were collected simultaneously. The resultant joint force and torque at the hip, knee, ankle and shoulder for two trials per subject per condition were computed and normalized. Average kinematic, resultant joint force and torque data were compared using repeated-measures analysis of variance. Larger values were recorded for the vertical velocity of the centre of mass at take-off in the jumps with (mean 2.75, $s = 0.3 \text{ m} \cdot \text{s}^{-1}$) versus without (mean 2.44, $s = 0.23 \text{ m} \cdot \text{s}^{-1}$) an arm swing. The jumps with no arm swing produced larger torques at the hip during the first third of the propulsive phase (from zero to maximum vertical velocity of the centre of mass). During the final two-thirds of the propulsive phase, the arm swing augmented hip extensor torques by slowing the rate of trunk extension and placing the hip extensor muscles in slower concentric conditions that favoured the generation of larger forces and resultant joint torques. During the first two-thirds of the propulsive phase, knee extensor torque increased by 28% in the jumps with an arm swing, but maintained a relatively constant magnitude in the jumps with no arm swing.

Keywords: hip, joint torque, jumping, kinematics, kinetics, knee.

Introduction

Vertical jumping is a vital skill component in many sports and recreational activities. When performing a maximum height vertical jump, most athletes use a preparatory countermovement that results in a coordinated flexion of the hips, knees and ankles and a subsequent rapid extension of these same articulations before take-off. In most jumps, a rapid arm swing occurs simultaneously with the leg motions. Several investigators have demonstrated that a countermovement increases the height of a vertical jump (Enoka, 1988; Khalid *et al.*, 1989; Harman *et al.*, 1990), as it increases the 'pre-load' on the lower extremity musculature (Enoka, 1988; Anderson and Pandey, 1993; Zajac, 1993) and enables these muscles to utilize the stretch-shortening dynamics of muscular contraction (Cavagna *et al.*, 1968; Asmussen and Bonde-Peterson, 1974; Komi and Bosco, 1978; Enoka, 1988; Anderson and Pandey, 1993; Zajac, 1993). Additionally, the counter-

movement increases the time that the body has a positive upward acceleration (Harman *et al.*, 1990; Zajac, 1993). Research has also indicated that an arm swing increases jump height during countermovement vertical jumps (Luhtanen and Komi, 1978; Payne *et al.*, 1968; Khalid *et al.*, 1989; Oddson, 1989; Shetty and Etnyre, 1989; Harman *et al.*, 1990). However, the mechanisms that enable the arms to increase jump height are not well understood.

A deterministic model of vertical jumping (Hay and Reid, 1988) is presented in Fig. 1. Jump height, the height of the centre of mass of the body at its peak, is a function of the height of the centre of mass of the body at take-off and flight height, the vertical displacement of the centre of mass of the body while airborne. During a vertical jump, an arm swing that results in a body position of extreme shoulder flexion and elbow extension at take-off (i.e. arms extended and raised above the head) will increase the take-off height of the centre of mass of the body, resulting in an increased jump height. However, the motions of the arms may also affect the magnitude of the vertical component of the ground reaction force and enhance the propulsive and

* Author to whom all correspondence should be addressed. e-mail: mfeltner@pepperdine.edu

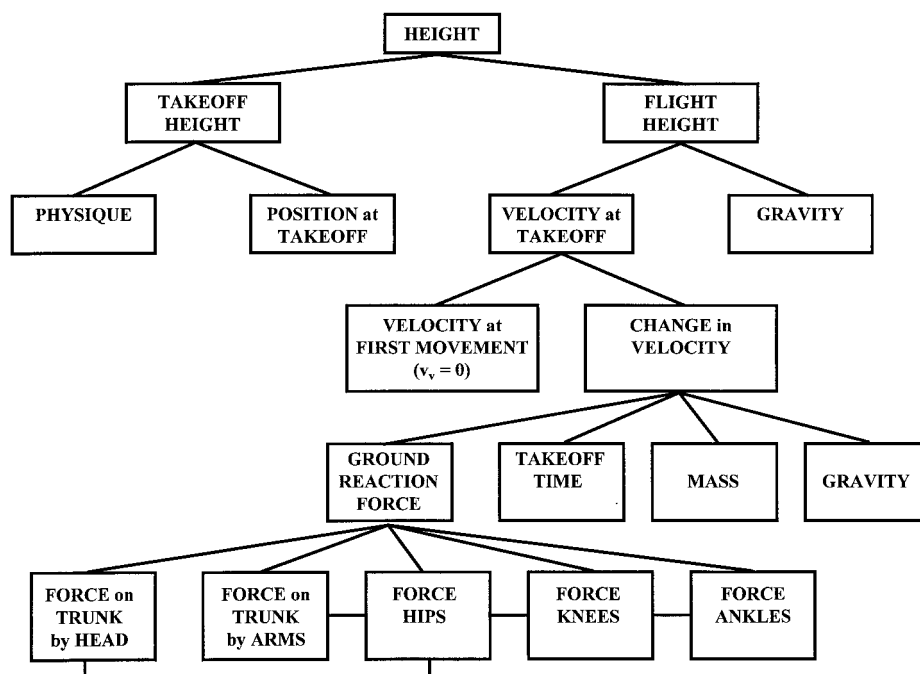


Figure 1 Deterministic model of the vertical jump adapted from Hay and Reid (1988).

net impulses exerted on the jumper. In turn, the larger net impulse would result in increased vertical velocity of the centre of mass of the body at take-off and augmented flight height (Fig. 1).

Payne *et al.* (1968) suggested that the arm swing enhances the magnitude of the vertical component of the ground reaction force immediately before take-off. During vertical jumping, Miller (1976) found that the net force exerted on both the body and trunk exhibited a 'double-peaked' or quartic trend consisting of two maxima surrounding a local minimum. She suggested that the arm motion reduced the magnitude of the maxima values, but increased the magnitude of the local minimum, and had an overall effect of increasing jump height. When the musculature of the lower extremity was in an 'advantageous position to exert vertical ground reaction force' (Harman *et al.*, 1990, p. 832), the upward acceleration of the arms (associated with the arm swing) was seen to create a downward force on the body at the shoulders that slowed the rate of shortening of the quadriceps and gluteal muscles. According to the force-velocity relationship for muscular contraction (Hill, 1938; Perrine and Edgerton, 1978), slower concentric actions of the leg muscles would result in enhanced muscle tension and presumably larger vertical ground reaction forces. However, no experimental data were provided to validate this mechanism.

The aim of this study was to examine the kinematics and kinetics of the body during countermovement vertical jumps performed both with and without an arm

swing. Specifically, the study sought to determine if an arm swing can augment the ability of the lower extremity musculature to generate tension, as measured by the resultant joint torques at the hip, knee and ankle.

Methods

Participants

Twenty-five members (14 males, 11 females) of the 1995 Pepperdine University men's and women's volleyball teams (males: height, mean 193.8, $s = 6.1$ cm; body mass, mean 88.2, $s = 6.6$ kg; age, mean 20.5, $s = 1.7$ years; women: height, mean 173.7, $s = 8.8$ cm; body mass, mean 69.3, $s = 7.1$ kg; age, mean 18.5, $s = 0.7$ years) provided voluntary written informed consent and served as participants. Each participant was videotaped performing five trials of countermovement vertical jumps from a force platform both with and without a bilateral arm swing. Before performing the jumps, each participant was given detailed instructions and allowed a brief period of practice. All jumps were initiated from a stationary upright posture and, during the jumps with no arm swing, the hands remained on the subject's iliac crests. The order of the jumps was randomized and 1–2 min rest was allowed between trials. The first two trials per condition that were performed correctly were used for the subsequent analyses.

Procedures

Before videotaping, several anthropometric measures were obtained to compute moment of inertia data (Hinrichs, 1985). Retroreflective markers were placed on nine body landmarks: centre of the head and the right shoulder, elbow, wrist, hip, knee, ankle, heel and toe. Assuming bilateral symmetry, these markers defined a six-segment model of the body: head and trunk, upper arm, forearm and hand, thigh, shank, and foot. The distance between the knee and ankle markers was also measured to scale the video images.

Owing to physical limitations within the laboratory, the distance between the camera and the participants was limited to 1.35 m and two video cameras were required to record the motions of the participants. The cameras were positioned on the right side of the participants with their optical axes oriented perpendicular to the sagittal plane of the athletes. Camera 1 was located at a height of 0.72 m and camera 2 at a height of 2.47 m. The cameras were genlocked to synchronize their instants of exposure and their respective fields of view overlapped by approximately 30 cm. Thus the two cameras (shutter speeds 1/1000 s; sampling rate 60 Hz) provided a field of view (approximately 1.5 × 3.5 m) large enough to record the motions of the participants.

Coordinates (in pixels) representing the location of the body landmarks were obtained using an automated digitizing process (Peak Performance Technologies, Englewood, CO) at instants ('output frames') separated by 1/60 s. To minimize perspective errors associated with the short distance between the camera and the participants, preliminary scale factors for the two cameras (SC_{1P} and SC_{2P} , respectively) were determined using a metre-stick placed in the approximate plane of motion of the athlete. At the instant of each output frame, the scale factor for camera one (SC_1) was computed as follows:

$$SC_1 = l_{SK} \text{ (m)} / l_{SK} \text{ (pixels)} \quad (1)$$

where l_{SK} is the distance between the knee and the ankle markers. The scale factor for camera 2 (SC_2) was then computed using SC_1 and the ratio between SC_{2P} and SC_{1P} :

$$SC_2 = SC_1 (SC_{2P} / SC_{1P}) \quad (2)$$

As the shank is in the plane of movement, computing camera scale factors at the instant of each output frame eliminated the effects of perspective error in the calculation of the scaled coordinates for all landmarks except the elbow and wrist. The effects of perspective errors on the scaled coordinates of the elbow and wrist were minimized by ensuring that the participants swung their arms in a sagittal plane adjacent and parallel to the plane

of motion of the other body landmarks. All coordinate data were examined for discontinuities as the landmarks moved between the fields of view of the two cameras. No discontinuities were noted.

At the instant of each output frame, the coordinates (in metres) of each landmark were computed as the product of its digitized coordinates (in pixels) and the appropriate scale factor (SC_1 or SC_2). All coordinates were expressed in terms of an orthogonal laboratory-based inertial reference frame R_0 . The axes of R_0 (X_0 , Y_0 and Z_0) were defined by unit vectors i_0 , j_0 and k_0 , respectively. Vector k_0 pointed vertically upward; j_0 was horizontal and pointed anteriorly; i_0 was horizontal and pointed to the participant's right side.

Simultaneous with the recording of the videotape information, ground reaction force and centre of pressure data were collected from a Kistler force plate (Model 9281B) at a sampling rate of 1000 Hz using Bioware software (Kistler Instrument Company, Amherst, NY). The correspondence between the video and force plate data was determined using a video synchronization unit (Peak Performance Technologies) that simultaneously displayed a marker in the video image and transmitted an analog signal to the Bioware software. In all trials, the instant of take-off was determined as the instant the vertical component of the ground reaction force dropped below 4 N. A time of 10.00 s was assigned to the instant of take-off.

The varied sampling rates for the landmark coordinates (60 Hz) and the ground reaction force and centre of pressure data (1000 Hz) necessitated computation of average ground reaction force and centre of pressure values at the instant of each output frame. This was accomplished using the equation:

$$\bar{Q}(t) = \frac{1}{t_f - t_f/2} \int_{t_f - t_f/2}^{t_f + t_f/2} Q(i) dt \quad (3)$$

where t is the time of the videotape output frame, $\bar{Q}(t)$ is the value of the respective ground reaction force or centre of pressure component at the instant of each output frame, $Q(i)$ is the instantaneous value of the respective ground reaction force or centre of pressure component determined from the force plate, and t_f is the time between each output frame (1/60 s). At the instant of each output frame, the respective ground reaction force and centre of pressure components were expressed in terms of reference frame R_0 .

Data smoothing

The time-dependent coordinates of each body landmark were smoothed using a quintic spline smoothing routine (Wood and Jennings, 1979; Vaughan, 1980) to reduce small random errors that may have occurred

during digitizing. To determine the smoothing factor for each trial, the vertical acceleration of the body's centre of mass (G) at the instant of each output frame [$a_{zG-FP}(i)$] was computed using the following equation:

$$a_{zG-FP}(i) = (F_Z(i) - mg)/m \quad (4)$$

where $F_Z(i)$ is the value of the vertical component of the ground reaction force at the instant of each output frame, m is the mass of the subject and g is gravitational acceleration. Using an iterative procedure, the smoothing factor was increased in 2.0×10^{-6} increments and the vertical acceleration of the body's centre of mass based upon the digitized landmark coordinates (a_{zG-COR}) was computed (Dapena, 1978; see following section). For each value of the smoothing factor, the average residual (\bar{r}) between a_{zG-COR} and a_{zG-FP} for the trial was computed:

$$\bar{r} = \frac{1}{n} \sum_{i=1}^n |a_{zG-COR}(i) - a_{zG-FP}(i)| \quad (5)$$

where n is the number of output frames in a trial. The smoothing factor value that minimized \bar{r} was selected for each trial. For the jumps with an arm swing, the mean smoothing factor was 9.2 ($s = 5.5$) $\times 10^{-6}$ per frame in the Y_0 and Z_0 directions and the average \bar{r} -value was 0.91 ($s = 0.26$) $m \cdot s^{-2}$. For the jumps without an arm swing, the mean smoothing factor was 7.6 ($s = 7.4$) $\times 10^{-6}$ per frame in the Y_0 and Z_0 directions and the average \bar{r} -value was 0.83 ($s = 0.30$) $m \cdot s^{-2}$. The smoothed two-dimensional landmark data expressed in terms of reference frame R_0 were used for all subsequent computations.

Linear kinematics

The linear velocity (v) and acceleration (a) of each landmark were computed as the first and second derivatives, respectively, of quintic spline functions fitted to the time-dependent components of the landmark coordinates. The displacement (s), velocity and acceleration of segmental centres of mass were computed using the equation presented by Dapena (1978) and centre of mass location data reported by Clauser *et al.* (1969) and adjusted according to Hinrichs (1990). The displacement, velocity and acceleration of the body's centre of mass (s_G , v_G and a_G , respectively) were also computed using the procedures detailed by Dapena (1978). Equations similar to those used to compute s_G , v_G and a_G were also used to compute the displacement, velocity and acceleration of the following segments: arms, legs, head and trunk, and head, trunk and arms. The relative accelerations of the segments were computed using the general equation:

$$a_{s1/s2} = a_{s1} - a_{s2} \quad (6)$$

where $a_{s1/s2}$ is the acceleration of segment 1 relative to segment 2, and a_{s1} and a_{s2} are the absolute accelerations of segments 1 and 2, respectively.

Angular kinematics

The absolute angular orientation (θ) of the extremity segments were computed using the general equation:

$$\theta = \cos^{-1}(\mathbf{r}_{\text{PROXIMAL/DISTAL}} \cdot \mathbf{j}_0) \quad (7)$$

where $\mathbf{r}_{\text{PROXIMAL/DISTAL}}$ is a unit vector pointing from the distal to proximal endpoint of the segment and the symbol \cdot indicates the dot product operation. The absolute angular orientation of the trunk (θ_{TR}) was:

$$\theta_{\text{TR}} = \cos^{-1}(\mathbf{r}_{\text{SHLD/HIP}} \cdot \mathbf{j}_0) \quad (8)$$

where $\mathbf{r}_{\text{SHLD/HIP}}$ is a unit vector pointing from the hip to the shoulder. The absolute angular velocity (ω) and acceleration (α) of each segment were computed as the first and second derivatives, respectively, of quintic spline functions fitted (zero smoothing) to the time-dependent θ -values.

Joint angles at the ankle (θ_{ANK}), knee (θ_{KNEE}) and hip (θ_{HIP}) were computed using the following equations:

$$\theta_{\text{ANK}} = \pi + \theta_{\text{FT}} - \theta_{\text{SK}} \quad (9)$$

$$\theta_{\text{KNEE}} = \theta_{\text{TH}} - \theta_{\text{SK}} \quad (10)$$

$$\theta_{\text{HIP}} = \pi - \theta_{\text{TR}} + \theta_{\text{TH}} \quad (11)$$

where θ_{FT} , θ_{SK} , θ_{TH} and θ_{TR} are the angular orientations of the foot, shank, thigh and trunk, respectively. The angular velocity at each joint was computed as the first derivatives of quintic spline functions fitted (zero smoothing) to the time-dependent joint angle (θ) values. Signs and reference values for the segment and joint angles are displayed in Fig. 2.

Joint kinetics

Inverse dynamics (Andrews, 1974, 1982; Feltner and Dapena, 1986) were used to compute the proximal resultant joint force and resultant joint torque exerted at the ankle, knee, hip and shoulder. For the lower extremity, the foot was modelled as being subjected to a proximal resultant joint torque (T_{ANK}) and three forces: the ground reaction force applied at the centre of pressure, weight at its centre of mass, and a proximal resultant joint force (F_{ANK}). The shank and thigh were each assumed to be subjected to a proximal resultant joint torque (T_{KNEE} or T_{HIP} , respectively), a distal resultant joint torque, and three forces: weight at its centre of mass, a proximal resultant joint force (F_{KNEE} or F_{HIP} ,

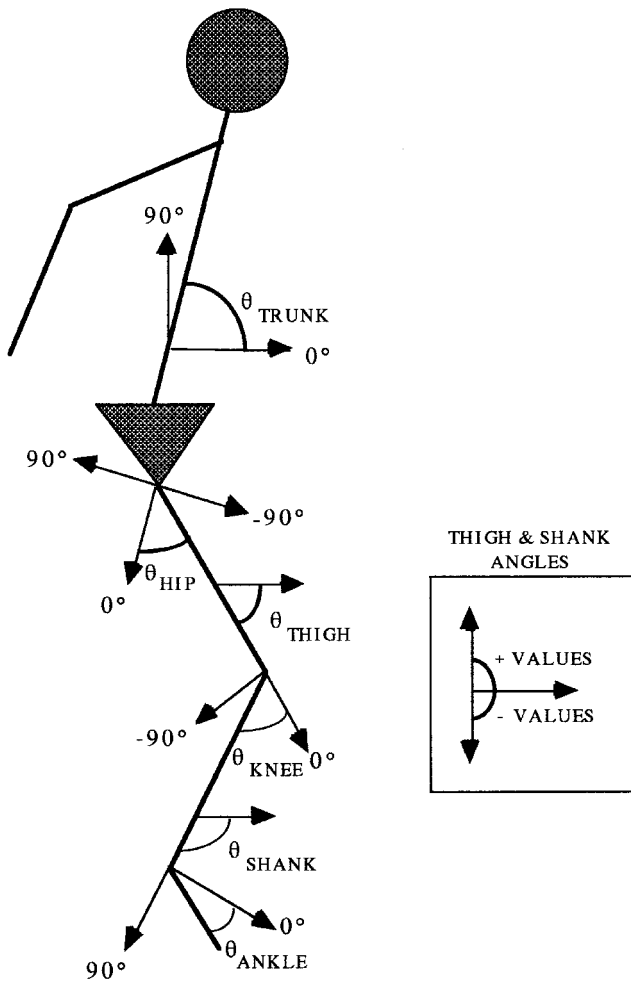


Figure 2 Signs and reference values for the angular kinematic data.

respectively) and a distal resultant joint force. For the upper extremity, the forearm and hand segment was assumed to be subjected to weight acting at its centre of mass and a proximal resultant joint force and resultant joint torque. The upper arm was modelled as being acted upon by a proximal resultant joint torque (T_{SHLD}), a distal resultant joint torque and three forces: weight acting at its centre of mass, a proximal resultant joint force (F_{SHLD}) and a distal resultant joint force. The moment of inertia values about the transverse axis of each segment reported by Chandler *et al.* (1975) were used and personalized for each participant (Hinrichs, 1985).

The proximal resultant joint force ($RJF_{PROXIMAL}$) exerted on a segment was computed using the general equation:

$$RJF_{PROXIMAL} = m(a_{CM} - g) - F_{DISTAL} \quad (12)$$

where a_{CM} and g are the accelerations of the segment's centre of mass and gravity, respectively, and F_{DISTAL} is

the distal force applied to the segment (if applicable). The local angular momentum of each segment about a transverse axis through its centre of mass was computed using a modification of the procedures presented by Dapena (1978). The net torque (ΣT) on each segment about its centre of mass was calculated as the first derivative of its local angular momentum. The proximal resultant joint torque ($RJT_{PROXIMAL}$) exerted on a segment was then computed using the general equation:

$$RJT_{PROXIMAL} = \Sigma T - RJT_{DISTAL} - T_{FPROXIMAL} + T_{FDISTAL} \quad (13)$$

where RJT_{DISTAL} is the distal resultant joint torque applied to the segment (if applicable), and $T_{FPROXIMAL}$ and $T_{FDISTAL}$ are the torques created about the segment's centre of mass by the proximal and distal resultant joint forces applied to the segment (if applicable). Positive torque values result in extension of the trunk, hip and knee, and plantar flexion at the ankle.

Data analysis

To aid the interpretation of the kinetic and kinematic data, the jump was divided into four periods (A–D) using five instants (see Fig. 3): (1) t_{FM} , the time of first movement was subjectively determined as the instant the magnitude of the vertical component of the ground reaction force decreased approximately 5 N below the participant's body weight; (2) t_{NV} , the instant of maximum negative vertical velocity of the centre of mass; (3) t_{LP} , the instant of minimum vertical displacement of the centre of mass of the body; (4) t_{PV} , the instant of maximum positive vertical velocity of the centre of mass of the body; and (5) t_{TO} , the instant of take-off. At t_{NV} and t_{PV} , the vertical acceleration of the body's centre of mass (a_{zG}) equals zero. Therefore, the following general equation was used to compute t_{NV} and t_{PV} :

$$t_{INT} = t(i) + \left(\frac{-a_{zG}(i)}{(a_{zG}(i+1) - a_{zG}(i))} \right) t_f \quad (14)$$

where t_{INT} is the interpolated time value (t_{NV} or t_{PV}), t is time, t_f is the time between each output frame, and i and $i+1$ indicate the output frames immediately before and after the instant when a_{zG} equals zero. At the instant of t_{LP} , the vertical velocity of the centre of mass of the body (v_{zG}) equals zero. Therefore, the following general equation was used to compute t_{LP} :

$$t_{LP} = t(i) + \left(\frac{-v_{zG}(i)}{(v_{zG}(i+1) - v_{zG}(i))} \right) t_f \quad (15)$$

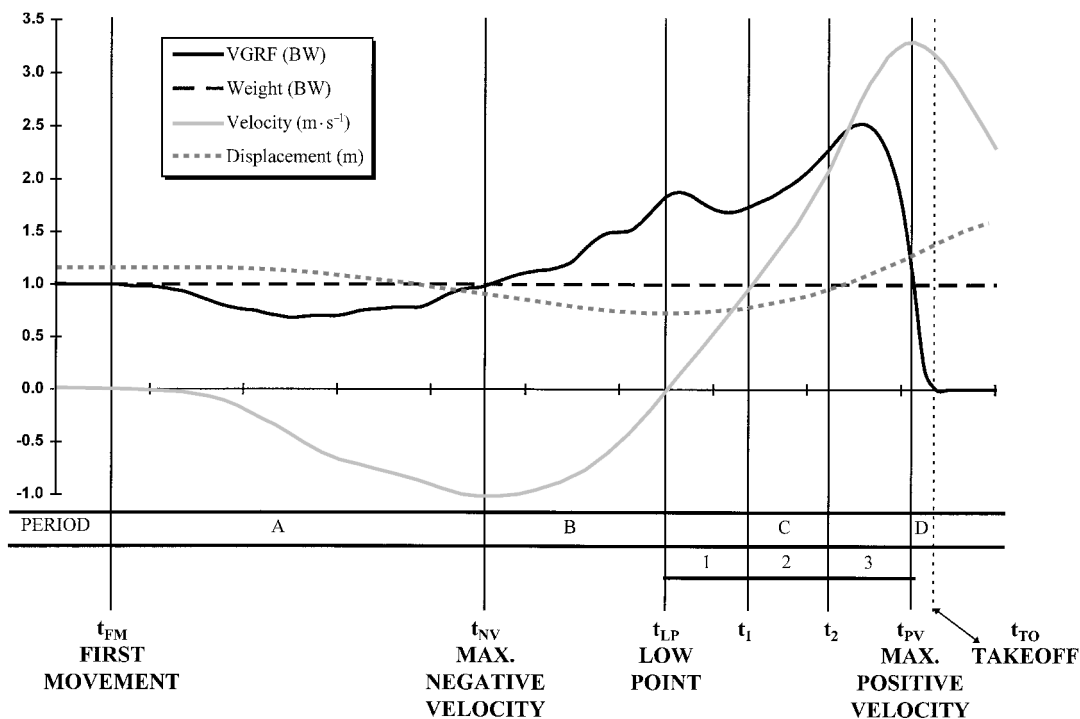


Figure 3 Sketch depicting the periods used to analyse the vertical jumps.

To examine further the jumps with and without an arm swing, the propulsive phase (period C) was divided into three sub-periods (C_1 , C_2 and C_3) of equal time by defining the instants t_1 and t_2 , where $t_1 = t_{LP} + 1/3(t_{PV} - t_{LP})$ and $t_2 = t_{LP} + 2/3(t_{PV} - t_{LP})$ (see Fig. 3).

For each period A–D and each sub-period C_1 – C_3 , the average values of joint torques, forces and angular velocities were computed using an equation of the general form:

$$\bar{Q} = \frac{1}{t_{\text{PERIOD}}} \int_{t_A}^{t_B} Q(i) dt \quad (16)$$

where t_{PERIOD} is the duration of the period; t_A and t_B are the times that define the start and end of the period, respectively; \bar{Q} is the average value of the data parameter during the period; and $Q(i)$ indicates the instantaneous values of the respective data parameters. All force values were normalized by dividing by the participant's weight and are reported in body weight units. All torque values were normalized by dividing by the product of the participant's mass and height squared ($\text{mass} \times \text{height}^2$).

One-way repeated-measures analyses of variance (Keppel, 1982) were used to compare the discrete biomechanical data for the jumps with versus without an arm swing. Owing to the large number of statistical comparisons ($n = 117$) and in an effort to avoid Type I errors, the experiment-wide error rate was established *a priori* at $P \leq 0.05$ using a Bonferroni correction

(Keppel, 1982). This resulted in a per comparison α of $P \leq 0.0005$. However, the Bonferroni correction will result in an increased Type II error rate. Examination of the statistical results indicated that in 16 cases the probability associated with the per comparison F -ratio was greater than $P \leq 0.0005$, but less than $P \leq 0.05$. These cases have been indicated in Tables 1–6. As the aim of the study was to identify factors that clearly discriminated between the jumps with and without an arm swing, the more stringent experiment-wide error rate of $P \leq 0.05$ was used to determine statistical significance during data analysis.

To present ensemble average curves for the arm-swing and no-arm-swing groups, the times during each jump [$t(i)$] were normalized and expressed as a function of the length of the propulsive phase (period C):

$$\%t(i) = \left[\frac{t(i) - t_{LP}}{t_{PV} - t_{LP}} \right] \times 100 \quad (17)$$

where $\%t(i)$ is the normalized time at the instant of output frame i . Quintic spline functions (zero smoothing) were then fitted to the time-normalized-dependent kinetic and kinematic data. The spline functions were used to compute interpolated values at 5% increments from an instant after the time of first movement (–150%) until an instant after take-off (130%). The normalized values for all subjects in the arm-swing and no-arm-swing groups were then averaged at each $\%t(i)$ value.

Table 1 Linear kinematic data for body and segment centres of mass and temporal data (mean \pm s)

	Arm swing	No arm swing
min. s_{zG} (%) ^a	40.9 \pm 3.3	38.4 \pm 3.9 ^d
s_{zG} at take-off (%) ^a	71.1 \pm 1.7	67.8 \pm 1.8 ^d
v_{zG} at take-off (m \cdot s ⁻¹)	2.75 \pm 0.28	2.44 \pm 0.23 ^d
max. $-v_{zG}$ (m \cdot s ⁻¹)	-1.16 \pm 0.32	-1.26 \pm 0.31 ^e
max. a_{zG} (m \cdot s ⁻²)	14.4 \pm 2.8	12.4 \pm 2.2 ^d
max. a_{zARM} (m \cdot s ⁻²)	82.4 \pm 16.8	18.6 \pm 4.6 ^d
max. a_{zHT} (m \cdot s ⁻²)	18.0 \pm 3.4	15.9 \pm 3.0 ^d
max. a_{zHTA} (m \cdot s ⁻²)	18.3 \pm 3.8	15.9 \pm 3.0 ^d
time v_{zG} equals zero (t_{LP}) (s)	9.68 \pm 0.04	9.67 \pm 0.04
time t_1 (s) ^b	9.77 \pm 0.03	9.76 \pm 0.03
time t_2 (s) ^c	9.87 \pm 0.02	9.86 \pm 0.02
time of max. positive v_{zG} (t_{PV}) (s)	9.96 \pm 0.01	9.96 \pm 0.01
time of take-off (t_{TO}) (s)	10.00 \pm 0.00	10.00 \pm 0.00

s_{zG} = vertical linear displacement of the centre of mass of the body (G); v_{zG} = vertical linear velocity of the centre of mass of the body; a_{zG} = vertical linear acceleration of the centre of mass of the body; a_{zARM} = vertical linear acceleration of the centre of mass of the arm segment (ARM); a_{zHT} = vertical linear acceleration of the centre of mass of the head and trunk segment (HT); a_{zHTA} = vertical linear acceleration of the centre of mass of the head, trunk and arm segment (HTA).

^a Percentage of standing height; ^b $t_1 = t_{LP} + 1/3 (t_{PV} - t_{LP})$; ^c $t_2 = t_{LP} + 2/3 (t_{PV} - t_{LP})$.

^d Experiment-wide $P \leq 0.05$ (per comparison $P \leq 0.0005$). ^e Per comparison $P \leq 0.05$.

Results and discussion

The jumps with an arm swing had a larger vertical velocity of the body centre of mass (v_{zG}) at take-off and the body's centre of mass was located at a higher relative position above the ground (Table 1). As jump height is determined entirely by the height of the body's centre of mass and its vertical velocity at the instant of take-off (Fig. 1), these two factors resulted in higher jump heights for the arm-swing versus no-arm-swing jumps. The arm swing raised the body's centre of mass by 3% of standing height at take-off relative to the jumps with no arm swing (an average increase of 6.1 cm for the height of the centre of mass at take-off) (Table 1). The vertical velocity of the body's centre of mass at take-off was 12.7% larger in the arm-swing versus no-arm-swing jumps (Table 1) and would result in an increase of 8.2 cm in the vertical displacement of the body's centre of mass between take-off and the peak of the jump. Thus the arm swing added approximately 14.3 cm to the peak height of the body's centre of mass during a vertical jump; 43% of the increase in jump height was due to the arms being in a raised position at take-off and 57% of the increase was due to effects associated with the arm motion that occurred before take-off. For an average athlete (height = 186 cm), peak height of the centre of mass of the body would have been 171 cm in the jumps with an arm swing and 156 cm in the jumps without an arm swing. Thus, arm motion increased peak jump

height by approximately 9%. This is in accordance with the findings of Luhtanen and Komi (1978), Shetty and Etnyre (1989) and Harman *et al.* (1990), who reported increases in take-off velocity of 10–11% in counter-movement vertical jumps using an arm swing, and those of Payne *et al.* (1968) and Khalid *et al.* (1989), who reported a 5–10% increase in jump height in counter-movement vertical jumps performed using an arm swing. However, the 21% increase in take-off velocity reported by Oddson (1989) was not substantiated.

The jumps with an arm swing exhibited larger maximal vertical accelerations for the centre of mass of the body, arms, head and trunk, and head, trunk and arms segments (Table 1; Figs 4 and 5). In the arm-swing jumps, the arm swing resulted in a large positive (upward) vertical acceleration of the arms relative to the trunk throughout most of periods C_1 and C_2 ($a_{zARM/HT}$ in Fig. 4). For the arms to acquire a positive vertical acceleration, the trunk must make positive vertical forces on the arms at the shoulder (F_{SHLD}). By reaction, the arms make negative (downward) vertical forces on the trunk at the shoulder ($F_{TR(SHLD)}$) during periods C_1 and C_2 .

During the arm-swing jumps, the vertical acceleration of the head and trunk segment (a_{zHT}) exhibited a quartic trend: it reached local maxima near the instant of minimum vertical displacement of the centre of mass (t_{LP}) and t_2 , and a local minimum at t_1 when the acceleration of the arms relative to the head and trunk ($a_{zARM/HT}$) was

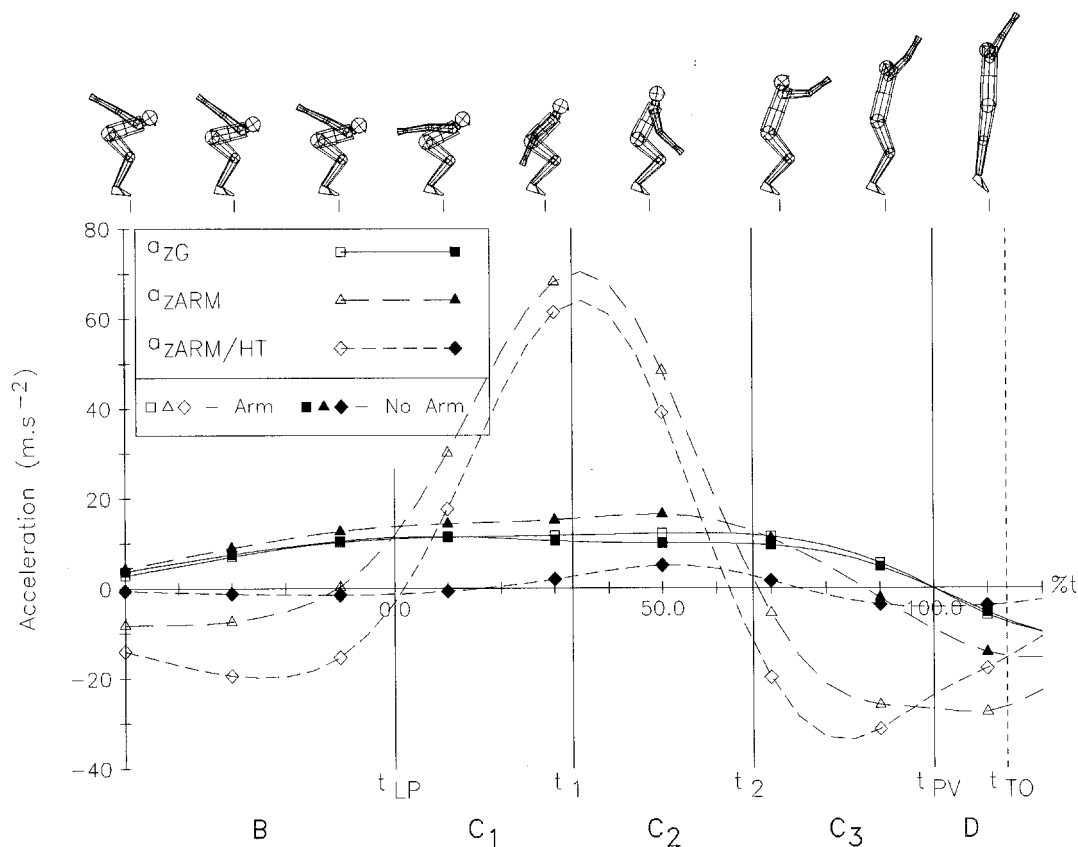


Figure 4 Ensemble averages of the vertical acceleration of the centre of mass of the body (a_{zG}), arms (a_{zARM}) and arms relative to the head and trunk ($a_{zARM/HT}$) for the arm-swing and no-arm-swing jumps. Time is expressed as the percentage of the propulsive phase (period C). The maximum negative velocity of the centre of mass of the body during the countermovement occurred near $t = -42\%$ and take-off occurred at $t = 113\%$ in both types of jump. The four solid vertical lines indicate the instants of t_{LP} , t_1 , t_2 and t_{PV} , respectively, and the dashed vertical line indicates the instant of take-off (t_{TO}). Periods B, C₁, C₂, C₃ and D are labelled below the graph. The sequence above the graph indicates the motions of a representative athlete performing an arm-swing jump.

at its maximal value (Figs 4 and 5). In the jumps without an arm swing, the vertical acceleration of the head and trunk (a_{zHT}) and the head, trunk and arm (a_{zHTA}) segments reached their maximum magnitudes near the instant of minimum vertical displacement of the centre of mass and decreased through take-off. In the jumps with an arm swing, despite the decrease in the magnitude of the vertical acceleration of the head and trunk near t_1 , the vertical acceleration of the head, trunk and arm segment reached its maximum value near t_1 and exhibited larger magnitudes relative to the jumps without an arm swing until near the midpoint of period C₃. As the head, trunk and arm segment accounts for over 70% of the mass of the body, larger magnitudes for its acceleration in the jumps with an arm swing resulted in larger magnitudes for the vertical acceleration of the centre of mass (a_{zG}) (Fig. 4).

Both types of jump used a preparatory countermovement. During vertical jumps, the vertical velocity of the centre of mass of the body at take-off is due entirely to the net vertical impulse exerted upon the

jumper between the instant of minimum vertical displacement of the centre of mass and take-off. For this reason, only this period was examined in detail when comparing the arm-swing and no-arm-swing jumps. As a jumper must have zero vertical velocity at the instant of minimum displacement, augmentation of jump height from a countermovement must result from changes in the 'state' of the musculature at t_{LP} or to changes in the neuromechanical properties of the musculature associated with the countermovement that persist after t_{LP} . Thus, examination of the period between t_{LP} and the instant of take-off would identify the mechanical factors that result in the vertical velocity of the centre of mass of the body at take-off, regardless of whether these factors are associated with the countermovement.

The net vertical impulse exerted on the jumper between the instant of minimum vertical displacement of the centre of mass and take-off is due to the net force made on the jumper and the time that the net force acts. As indicated by the temporal data (Table 1), the time between t_{LP} and the instant of take-off was nearly

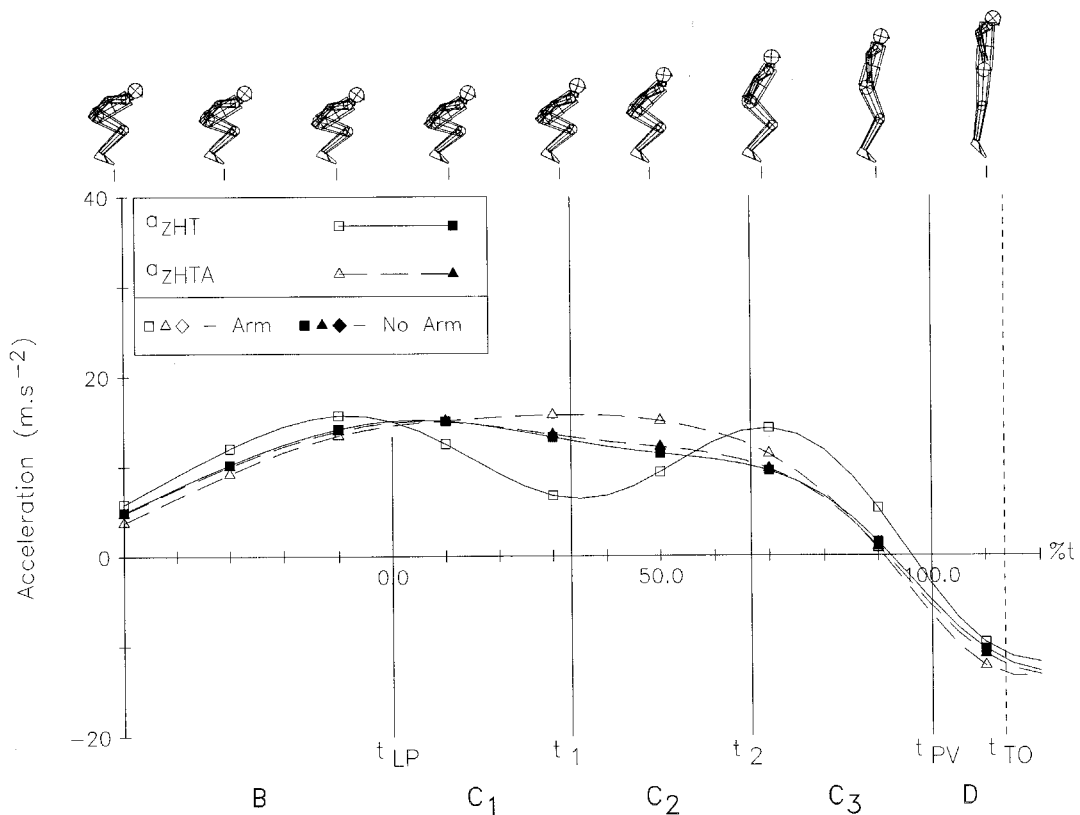


Figure 5 Ensemble averages of the vertical acceleration of the centre of mass of the head and trunk segment (a_{zHT}) and of the head, trunk and arm segment (a_{zHTA}) for the arm-swing and no-arm-swing jumps. Time is expressed as the percentage of the propulsive phase (period C). The four solid vertical lines indicate the instants of t_{LP} , t_1 , t_2 and t_{PV} , respectively, and the dashed vertical line indicates the instant of take-off (t_{TO}). Periods B, C_1 , C_2 , C_3 and D are labelled below the graph. The sequence above the graph indicates the motions of a representative athlete performing a no-arm-swing jump.

identical in the arm-swing and no-arm-swing jumps (arm-swing jumps: 0.32, $s = 0.04$ s; no-arm-swing jumps: 0.33, $s = 0.04$ s). Harman *et al.* (1990) also reported similar values for this period in the arm-swing and no-arm-swing jumps. Thus, differences in the net impulse exerted on the jumper in the arm-swing versus no-arm-swing jumps must be a result of changes in the vertical component of the ground reaction force (F_z in Table 2). As the ground reaction force results from the actions of the jumper, sequential examination of the kinetic and kinematic data between the instant of minimum vertical displacement and take-off should elucidate the causal mechanisms associated with the arm action that resulted in increased jump height.

Examination of the kinematic and kinetic data for the lower extremity indicated no significant differences in the kinematic and kinetic data associated with the ankle. Therefore, the following descriptions will not focus upon the ankle. Failure to discuss the ankle in the following sections does not imply a lack of importance for the musculature of the ankle in vertical jumping. Rather, the findings of the current investigation revealed

that the kinetics and kinematics of the ankle joint were not altered by the presence or absence of an arm swing.

Period C_1

At the start of the propulsive phase, the no-arm-swing jumpers were in positions of increased knee and hip flexion, but less forward trunk inclination, relative to the arm-swing jumpers (Table 3 and sequences in Figs 4 and 5). Both groups were rotating the trunk counter-clockwise at the instant of minimum vertical displacement of the centre of mass, but the arm-swing jumpers rotated the trunk at a faster rate (ω_{TR} in Fig. 6 and Table 4). The thigh was relatively motionless at the instant of minimum vertical displacement in both groups; thus, trunk rotation resulted in faster rates of hip extension for the arm-swing jumpers (ω_{TH} and ω_{HIP} in Fig. 6 and Table 4). At the start of the propulsive phase, the knees were continuing to flex at a low rate for both jump styles (ω_{KNEE} in Fig. 7 and Table 5) and the arms were beginning their upward acceleration relative to the trunk in the arm-swing jumps ($a_{zARM/HT}$ in Fig. 4). Lastly, the

Table 2 Instantaneous and average values (BW_s) for the vertical component of the ground reaction force (F_z) during period C. Instantaneous values are reported at the times of the four events (t_{LP} , t_1 , t_2 and t_{PV}) that define the subperiods of period C and average values are reported for the intervals C_1 , C_2 and C_3 . Instantaneous values ($m \cdot s^{-1}$) of the vertical velocity of the body centre of mass (v_{zG}) are also reported for the instants of t_{LP} , t_1 , t_2 and t_{PV} (mean \pm s)

	Arm swing		No arm swing	
	F_z	v_{zG}	F_z	v_{zG}
Instantaneous				
t_{LP}	2.0 ± 0.3^b	0.00 ± 0.00	2.1 ± 0.3^b	0.00 ± 0.00
t_1	1.9 ± 0.2	1.07 ± 0.16	1.9 ± 0.2	1.07 ± 0.14
t_2	2.3 ± 0.2^a	2.20 ± 0.18^a	1.9 ± 0.1^a	2.03 ± 0.16^a
t_{PV}	1.3 ± 0.2	2.93 ± 0.25^a	1.3 ± 0.2	2.66 ± 0.25^a
Average				
Period C_1	1.9 ± 0.2		2.0 ± 0.2	
Period C_2	2.1 ± 0.2^a		1.9 ± 0.2^a	
Period C_3	2.1 ± 0.1^a		1.9 ± 0.1^a	

^a Experiment-wide $P \leq 0.05$ (per comparison $P \leq 0.0005$). ^b Per comparison $P \leq 0.05$.

Table 3 Angular displacements ($^\circ$) of lower extremities and trunk (see Fig. 2 for signs and reference values) at take-off (t_{TO}) and the low point (t_{LP}) of the jump (mean \pm s)

	Arm swing	No arm swing
Hip		
t_{TO}	0 ± 7	-9 ± 6^a
t_{LP}	-105 ± 16	-116 ± 12^a
Knee		
t_{TO}	-6 ± 3	-9 ± 4^a
t_{LP}	-90 ± 10	-98 ± 13^a
Ankle		
t_{TO}	33 ± 6	34 ± 6
t_{LP}	-27 ± 6	-27 ± 5
Trunk		
t_{TO}	85 ± 4	81 ± 5^a
t_{LP}	35 ± 13	30 ± 9^a

^a Experiment-wide $P \leq 0.05$ (per comparison $P \leq 0.0005$).

resultant joint torques at the hip (T_{HIP}) and knee (T_{KNEE}) had larger extension values in the no-arm-swing versus arm-swing jumps at the instant of minimum vertical displacement (Fig. 8 and Tables 4 and 5).

Throughout period C_1 , the no-arm-swing jumpers increased the rate of counterclockwise trunk rotation, clockwise thigh rotation and the associated extension of the hip (Fig. 6 and Table 4). Consequently, the musculature at the hip went from near isometric conditions at the instant of minimum vertical displacement of the centre of mass to concentric conditions at t_1 . Since the

force-generating capacity of skeletal muscle decreases as the rate of concentric action increases (Cavagna *et al.*, 1968; Asmussen and Bonde-Peterson, 1974; Komi and Bosco, 1978), the extension torque at the hip decreased in the no-arm-swing jumps throughout period C_1 . For the arm-swing jumps, the trunk rotated rapidly counterclockwise after the instant of minimum vertical displacement of the centre of mass, but it reached its maximal rate of extension before t_1 and was decreasing its rate of counterclockwise rotation before the end of period C_1 . As the thigh rotated clockwise at a relatively slow rate during period C_1 in the arm-swing jumps, the decreasing rate of counterclockwise trunk rotation resulted in a decreasing rate of hip extension at t_1 (Fig. 6). Consequently, the extension torque at the hip decreased slightly throughout period C_1 and reached a local minimum value near t_1 (Fig. 8 and Table 4). At t_1 , the magnitudes of the extension torques at the hip were nearly identical in the jumps with and without an arm swing. However, the average hip extension torque during C_1 was greater in the jumps without than with an arm swing, owing to the slower average rate of hip extension in the no-arm-swing jumps during C_1 (Table 4).

Why did the trunk decrease its rate of counterclockwise rotation in the jumps with an arm swing during period C_1 ? As the arms accelerate upward relative to the trunk, they result in a larger downward vertical force on the trunk ($F_{TR(SHLD)}$; the reaction to F_{SHLD} in Table 6). In turn, this force creates a clockwise torque about the centre of mass of the trunk ($T_{TR(SHLD)}$) that tries to decrease the rate of counterclockwise trunk rotation. Near the instant of minimum vertical displacement of

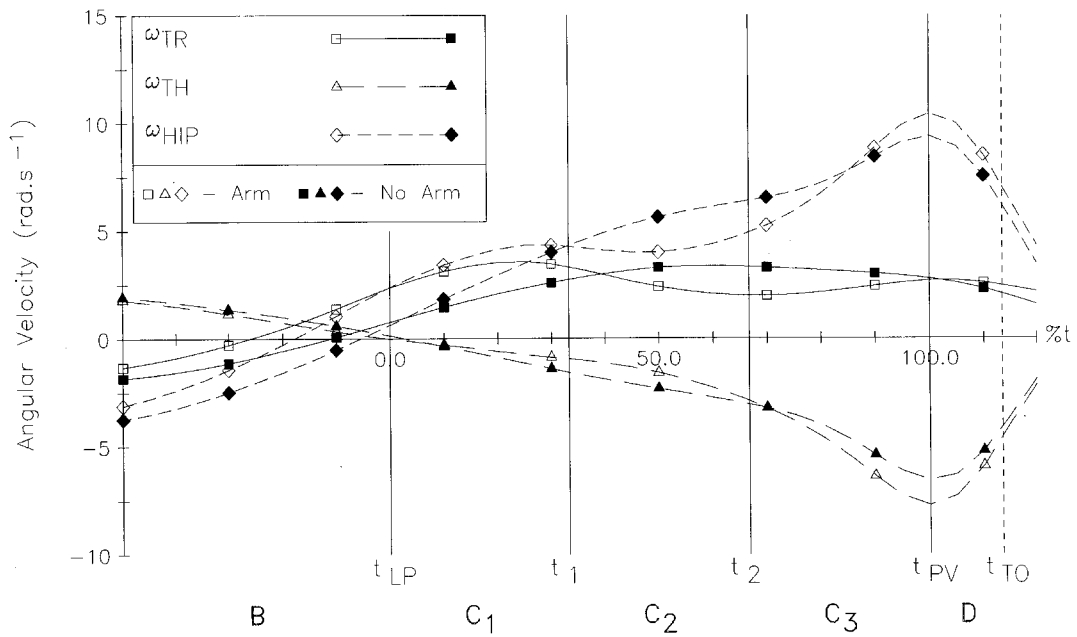


Figure 6 Ensemble averages of the angular velocity of the trunk (ω_{TR}), thigh (ω_{TH}) and hip (ω_{HIP}) for the arm-swing and no-arm-swing jumps. Extension values are positive for the hip; counterclockwise rotation values are positive for the trunk and thigh. Time is expressed as the percentage of the propulsive phase (period C). The four solid vertical lines indicate the instants of t_{LP} , t_1 , t_2 and t_{PV} , respectively, and the dashed vertical line indicates the instant of take-off (t_{TO}). Periods B, C_1 , C_2 , C_3 and D are labelled below the graph.

Table 4 Instantaneous and average angular velocities ($\text{rad} \cdot \text{s}^{-1}$) of the hip (ω_{HIP}), trunk (ω_{TR}) and thigh (ω_{TH}), and the instantaneous and average normalized joint torques ($\text{s}^{-2} \times 10$) at the hip (T_{HIP}) during period C. Instantaneous values are reported at the times of the four events that define the subperiods of period C (t_{LP} , t_1 , t_2 and t_{PV}) and average values are reported for the intervals C_1 , C_2 and C_3 (mean \pm s)

	Arm swing				No arm swing			
	ω_{TR}	ω_{TH}	ω_{HIP}	T_{HIP}	ω_{TR}	ω_{TH}	ω_{HIP}	T_{HIP}
Instantaneous								
t_{LP}	2.34 ± 1.17^a	-0.02 ± 0.42^b	2.36 ± 1.06^a	16.1 ± 2.6^a	0.75 ± 0.58^a	0.12 ± 0.23^b	0.63 ± 0.44^a	17.6 ± 3.3^a
t_1	3.30 ± 1.06^a	-0.96 ± 0.47^a	4.26 ± 1.12	14.8 ± 2.0	2.72 ± 0.93^a	-1.59 ± 0.40^a	4.31 ± 0.77	14.9 ± 1.5
t_2	1.99 ± 0.56^a	-2.91 ± 0.49^b	4.90 ± 0.77^a	14.5 ± 1.7^a	3.32 ± 0.61^a	-3.07 ± 0.47^b	6.39 ± 0.77^a	12.0 ± 1.3^a
t_{PV}	2.65 ± 0.59	-7.66 ± 0.82^a	10.31 ± 1.01^a	1.2 ± 1.6	2.76 ± 0.45	-6.53 ± 0.65^a	9.29 ± 0.80^a	1.6 ± 1.6
Average								
Period C_1	3.23 ± 1.01^a	-0.51 ± 0.42^a	3.72 ± 0.94^a	15.4 ± 2.0^a	1.82 ± 0.79^a	-0.72 ± 0.30^a	2.55 ± 0.59^a	16.6 ± 2.2^a
Period C_2	2.50 ± 0.75^a	-1.73 ± 0.47^a	4.21 ± 0.82^a	14.9 ± 1.8^a	3.18 ± 0.77^a	-2.34 ± 0.42^a	5.52 ± 0.77^a	13.4 ± 1.4^a
Period C_3	2.27 ± 0.42^a	-5.25 ± 0.49^a	7.52 ± 0.66^b	9.3 ± 1.2^a	3.09 ± 0.38^a	-4.63 ± 0.37^a	7.71 ± 0.52^b	8.4 ± 1.1^a

^a Experiment-wide $P \leq 0.05$ (per comparison $P \leq 0.0005$). ^b Per comparison $P \leq 0.05$.

the centre of mass, the downward vertical force exerted by the arms on the trunk is small and creates a negligible torque on the trunk (see Figs 9 and 10a). However, near t_1 , the centre of mass of the arms is close to its low point, the magnitude of the vertical component of the force on the trunk is increased, the magnitude of its horizontal component is near to zero, and the force creates a large

clockwise torque about the centre of mass of the trunk (Figs 9 and 10b). Thus, during the latter stages of period C_1 , the arm swing results in a decrease in the rate of counterclockwise trunk rotation. In turn, the decreased rate of counterclockwise trunk rotation slows the rate of hip extension. The decreasing rate of hip extension prevents the hip extensor muscles from

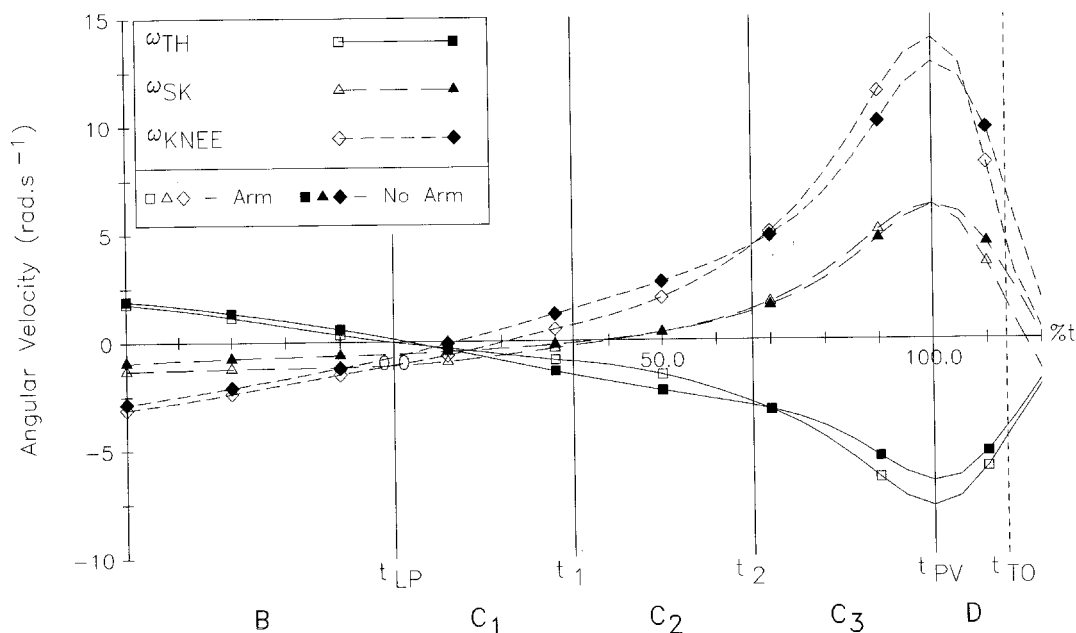


Figure 7 Ensemble averages of the angular velocity of the thigh (ω_{TH}), shank (ω_{SK}) and knee (ω_{KNEE}) for the arm-swing and no-arm-swing jumps. Extension values are positive for the knee; counterclockwise rotation values are positive for the thigh and shank. Time is expressed as the percentage of the propulsive phase (period C). The four solid vertical lines indicate the instants of t_{LP} , t_1 , t_2 and t_{PV} , respectively, and the dashed vertical line indicates the instant of take-off (t_{TO}). Periods B, C_1 , C_2 , C_3 and D are labelled below the graph.

Table 5 Instantaneous and average angular velocities ($\text{rad} \cdot \text{s}^{-1}$) of the knee (ω_{KNEE}), thigh (ω_{TH}) and shank (ω_{SK}), and the instantaneous and average normalized joint torques ($\text{s}^{-2} \times 10$) at the knee (T_{KNEE}) during period C. Instantaneous values are reported at the times of the four events that define the subperiods of period C (t_{LP} , t_1 , t_2 and t_{PV}) and average values are reported for the intervals C_1 , C_2 and C_3 (mean \pm s)

	Arm swing				No arm swing			
	ω_{TH}	ω_{SK}	ω_{KNEE}	T_{KNEE}	ω_{TH}	ω_{SK}	ω_{KNEE}	T_{KNEE}
Instantaneous								
t_{LP}	-0.02 ± 0.42^b	-1.10 ± 0.51^a	-1.08 ± 0.79^a	14.4 ± 4.4^a	0.12 ± 0.23^b	-0.58 ± 0.35^a	-0.70 ± 0.51^a	15.8 ± 3.9^a
t_1	-0.96 ± 0.47^a	-0.24 ± 0.45^b	0.72 ± 0.80^a	16.3 ± 3.0^b	-1.59 ± 0.40^a	-0.10 ± 0.44^b	1.47 ± 0.73^a	15.6 ± 2.0^b
t_2	-2.91 ± 0.49^b	1.41 ± 0.56	4.33 ± 0.87	18.5 ± 1.8^a	-3.07 ± 0.47^b	1.31 ± 0.42	4.38 ± 0.73	16.0 ± 1.7^a
t_{PV}	-7.66 ± 0.82^a	6.13 ± 0.87	13.77 ± 1.71^a	5.1 ± 1.9^a	-6.53 ± 0.65^a	6.13 ± 0.91	12.65 ± 1.29^a	6.7 ± 2.1^a
Average								
Period C_1	-0.51 ± 0.42^a	-0.73 ± 0.49^a	-0.23 ± 0.79^a	15.3 ± 3.4^b	-0.72 ± 0.30^a	-0.37 ± 0.40^a	0.35 ± 0.66^a	16.0 ± 2.7^b
Period C_2	-1.73 ± 0.47^a	0.44 ± 0.45	2.16 ± 0.77^a	17.6 ± 2.5^a	-2.34 ± 0.42^a	0.44 ± 0.37	2.78 ± 0.68^a	15.6 ± 1.9^a
Period C_3	-5.25 ± 0.49^a	3.84 ± 0.61^a	9.09 ± 0.98^a	14.7 ± 1.4^a	-4.63 ± 0.37^a	3.58 ± 0.52^a	8.20 ± 0.77^a	13.8 ± 1.4^a

^a Experiment-wide $P \leq 0.05$ (per comparison $P \leq 0.0005$). ^b Per comparison $P \leq 0.05$.

experiencing rapid concentric conditions and results in only a small decline in the hip extensor torque during period C_1 .

Miller (1976) reported that the angular acceleration of the trunk exhibited two periods of counterclockwise or extension angular acceleration (coinciding approximately with periods C_1 and C_3 in the current study) and an intermediate period of clockwise or flexion angular

acceleration (coinciding approximately with period C_2 in the current study) during arm-swing jumps. This pattern of trunk angular acceleration would be consistent with the angular velocity pattern exhibited for the trunk in the current study. Miller also found that the periods of counterclockwise trunk angular acceleration were associated with biceps femoris electromyographic activity.

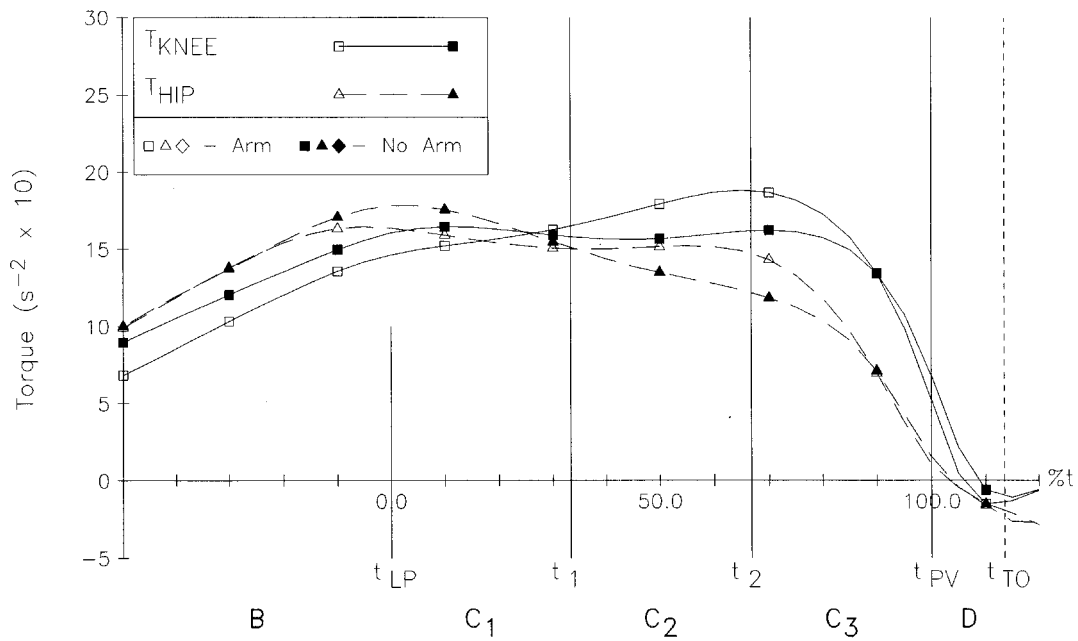


Figure 8 Ensemble averages of the torque at the knee (T_{KNEE}) and hip (T_{HIP}) for the arm-swing and no-arm-swing jumps. Extension torques have positive values. Time is expressed as the percentage of the propulsive phase (period C). The four solid vertical lines indicate the instants of t_{LP} , t_1 , t_2 and t_{PV} , respectively, and the dashed vertical line indicates the instant of take-off (t_{TO}). Periods B, C₁, C₂, C₃ and D are labelled below the graph.

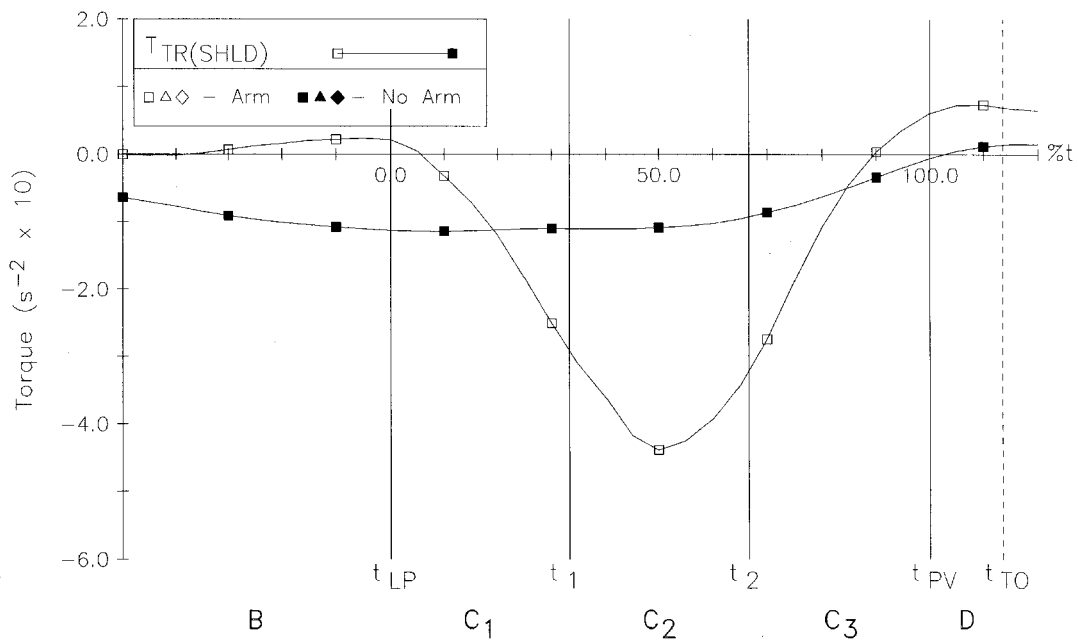


Figure 9 Ensemble averages of the torque created on the trunk by the arms ($T_{TR(SHLD)}$) for the arm-swing and no-arm-swing jumps. Time is expressed as the percentage of the propulsive phase (period C). The four solid vertical lines indicate the instants of t_{LP} , t_1 , t_2 and t_{PV} , respectively, and the dashed vertical line indicates the instant of take-off (t_{TO}). Periods B, C₁, C₂, C₃ and D are labelled below the graph.

The knee extensor muscles created larger torques at the instant of minimum vertical displacement of the centre of mass in the no-arm-swing versus arm-swing jumps (Table 5). It is unclear why the knee extensors

were creating larger torques at the instant of minimum vertical displacement in the jumps without an arm swing. However, it may be related to an increased stretch placed on the extensor group owing to the

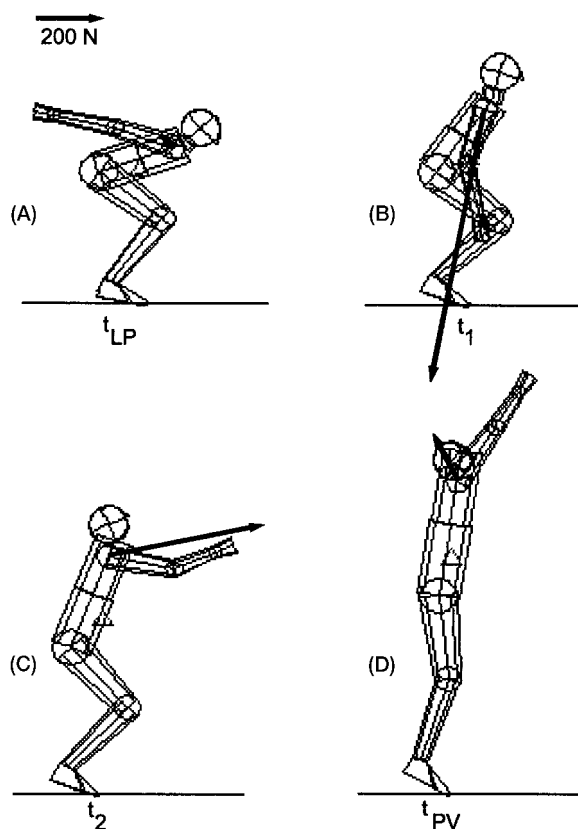


Figure 10 The positions of a representative athlete and $F_{TR(SHLD)}$ at instants near (A) t_{LP} , (B) t_1 , (C) t_2 and (D) t_{PV} . The triangle indicates the location of G.

increased flexion of the knee at the instant of minimum vertical displacement (Table 3) or to increased levels of activation of knee extensor motor units. During the preceding countermovement, the no-arm-swing jumpers had larger maximal negative values for the vertical velocity of the centre of mass (v_{zG}) (no-arm-swing jumps: mean maximum $-v_{zG} = -1.26$, $s = 0.31 \text{ m} \cdot \text{s}^{-1}$; arm-swing jumps: mean maximum $-v_{zG} = -1.16$, $s = 0.32 \text{ m} \cdot \text{s}^{-1}$), which may have required larger extensor torques at the knee to stop the downward motion of the body's centre of mass (Fig. 8, Table 1 and Table 5 at the instant of minimum vertical displacement).

Throughout period C_1 , the knee extensor torque maintained a relatively constant magnitude in the no-arm-swing jumps and increased in magnitude in the arm-swing jumps (Fig. 8 and Table 5) despite an increasing rate of knee extension during this period (Fig. 7 and Table 5). This may reflect volitional recruitment strategies used by the athletes or muscle tension benefits associated with the previous stretch of the quadriceps during the countermovement (Cavagna *et al.*, 1968; Asmussen and Bonde-Peterson, 1974; Komi and Bosco, 1978). It may also be associated with other neurophysiological and mechanical mechanisms

that continued to operate throughout period C_2 (see below).

At the end of period C_1 , vertical velocity of the centre of mass of the body was identical for both the arm-swing and no-arm-swing jumps (Table 2). However, the vertical accelerations of the centre of mass of the body (a_{zG}), the head and trunk segment (a_{zHT}), and the head, trunk and arm segment (a_{zHTA}), all reached their maximal values near the instant of minimum vertical displacement in the jumps without an arm swing and decreased in magnitude throughout period C_1 (Figs 4 and 5). Conversely, the vertical accelerations of the centres of mass of both the body and of the head, trunk and arm segment increased during period C_1 in the jumps with an arm swing despite a large decline in the acceleration of the head and trunk segment owing to the upward acceleration of the arms (Figs 4 and 5). The patterns of these three accelerations in period C_1 and throughout the jump were consistent with the results of Miller (1976).

Period C_2

In the jumps without an arm swing, the hip extended at increasingly faster rates during period C_2 (Fig. 6) and the rapid concentric conditions resulted in a continued decline in the magnitude of the hip extensor torque during this time (Fig. 8 and Table 4). In the jumps with an arm swing, the rate of hip extension initially declined during period C_2 , but exhibited a net increase relative to its value at t_1 by the instant of t_2 (Fig. 6 and Table 4). The changes in the rate of hip extension during the arm-swing jumps were primarily a result of the decreased rate of counterclockwise trunk rotation during period C_2 (Fig. 6 and Table 4). As the arm swing was responsible for decreasing the rate of counterclockwise trunk rotation, it resulted in slower average concentric conditions for the hip extensor musculature and was responsible for the increased hip extensor torque in the arm-swing versus no-arm-swing jumps during C_2 (Fig. 8 and Table 4). Near t_2 and as the vertical acceleration of the arms relative to the trunk was decreasing in the arm-swing jumps (Fig. 4), the magnitude of the torque exerted on the trunk ($T_{TR(SHLD)}$) began to decrease (Figs 9 and 10c). This halted the decline in the rate of counterclockwise trunk rotation (Fig. 6) and, together with the hip extensor torque, resulted in an increase in the rate of hip extension in the arm-swing jumps by t_2 .

In both the jumps with and without an arm swing, the knee extended at increasingly faster rates during period C_2 and was extending at approximately the same rate in both jump styles at t_2 (Fig. 7 and Table 5). The average extension angular velocity at the knee during period C_2 was significantly less in the jumps with an arm swing, and was associated with larger average knee extensor

torques in the arm-swing jumps than jumps without an arm swing during C_2 (Fig. 8 and Table 5). Despite an increasing rate of extension at the knee (implying faster concentric conditions) during period C_2 in both the arm-swing and no-arm-swing jumps, the normalized knee extensor torque (T_{KNEE}) increased in magnitude for both jump styles [no-arm-swing jumps: $\Delta T_{\text{KNEE}} = 0.4 \text{ s}^{-2} \times 10$ (2.5%); arm-swing jumps: $\Delta T_{\text{KNEE}} = 2.2 \text{ s}^{-2} \times 10$ (13.5%); Fig. 8 and Table 5].

The increase in extensor torque at the knee may be due to an increased moment arm for the quadriceps muscles. At t_1 , the knee was at approximately 90° of flexion in both jumps (arm swing: 91° ; no arm swing: 96°) and it extended approximately 15° during period C_2 (arm swing: 12° ; no arm swing: 16°). The moment arm for the quadriceps increases by 13–17% from 90° to 75° of extension (Smidt, 1973; Spoor and van Leeuwen, 1992) and could account for an increase in extensor torque. In the no-arm-swing jumps, the apparent increase in the moment arm for the quadriceps was offset by declining muscular forces throughout period C_2 and the extensor torque remained relatively constant during this interval. In the arm-swing jumps, the jumpers apparently used both an increase in moment arm and neurophysiological mechanisms that increased muscular tension to increase knee extensor torque.

The increases in knee extensor torque during both types of jump during period C_2 may be due to the action of the two-joint knee extensor (rectus femoris). As the hip was extending during C_2 , the rate of shortening of the rectus femoris would be less than that experienced by the vastii muscles of the quadriceps. The slower concentric conditions for the rectus femoris may be large enough to offset the declines in force owing to the faster concentric actions of the remaining quadriceps muscles during this period. Both Gregoire *et al.* (1984) and Bobbert and van Ingen Schenau (1988) reported that the rectus femoris exhibited high levels of electromyographic activity during this portion of no-arm-swing style jumps.

Changes in volitional levels of muscular activation and varying recruitment levels or discharge rates of the knee extensors during C_2 may also account for increased muscular tension in the quadriceps. During the countermovement, the no-arm-swing jumpers had a larger maximal negative value for the vertical velocity of the centre of mass of the body and they created larger extensor torques at the knee to stop the downward motion of the body's centre of mass (Fig. 8 and Table 5 at the instant of minimum vertical displacement). As a result and to stop the downward motion of the centre of mass of the body during the countermovement, jumps without an arm swing may require the recruitment of more extensor motor units or higher discharge rates of the active extensor motor units relative to jumps with

an arm swing. If the higher level of activation of the quadriceps during the countermovement results in short-term fatigue of the extensor motor units during the no-arm swing jumps, the size principle (Henneman, 1979) would dictate that fast-twitch, fatiguable motor units capable of producing large tensions would be de-recruited initially. Decreased activation of the fast-twitch, fatiguable motor units may result in a decreased ability of the quadriceps to generate tension during the propulsive phases of the no-arm-swing jumps. In turn, this may account for the lack of increase in the knee extensor torque, as the quadriceps moment arm was increasing during period C_2 in the no-arm-swing jumps.

Conversely for the jumps with an arm swing, the smaller knee extensor torques required during the countermovement may have allowed the jumpers to avoid recruitment of the fast-twitch, fatiguable motor units. As a result, activation of the fast-twitch, fatiguable motor units could be delayed until the periods during the propulsive phase of the jump when maximal knee extensor torque could be produced, resulting in the largest contribution to the vertical velocity of the centre of mass of the body. Thus, increased muscular forces produced by the quadriceps (despite increasing concentric conditions), coupled with an increasing moment arm for the quadriceps, could account for the increase in the knee extensor torque during periods C_1 and C_2 of the arm-swing jumps. Herzog *et al.* (1991) reported that maximal quadriceps force is produced at knee angles of approximately 78° , and Jensen *et al.* (1991) reported that maximal knee extensor torque following a preload occurs at approximately 75° of knee flexion. Collectively, this may suggest that, during the arm-swing jumps, recruitment of high-threshold, fast-twitch, fatiguable motor units is delayed until after the initiation of upward movement of the centre of mass of the body.

Additionally, as joint torques are indicative of the *net* muscular activity at an articulation (Andrews, 1974, 1982), the changes in the hip and knee extensor torques may be due to co-contraction of the agonist and antagonist muscle groups at the hip and knee. In both styles of jumps, the athletes need to produce hip and knee extensor torques during the propulsive phase of the jump. The hip extensor torque would be produced primarily by the gluteus maximus (one-joint muscle) and the hamstrings (two-joint muscle) and the knee extensor torque by the quadriceps. However, the two-joint hamstrings also create a flexion torque at the knee that would decrease the magnitude of the knee extensor torque produced by the quadriceps.

In the jumps without an arm swing, the gluteus maximus, hamstrings and quadriceps are active near their maximum levels at t_1 . However, as the athletes need to produce an extensor torque at the knee to continue the upward acceleration of the body during the

Table 6 Instantaneous and average force values (BW_s) at the hip (F_{HIP}), knee (F_{KNEE}), ankle (F_{ANK}) and shoulder (F_{SHLD}) during period C. Instantaneous values are reported at the times of the four events that define the subperiods of period C (t_{LP} , t_1 , t_2 and t_{PV}) and average values are reported for the intervals C₁, C₂ and C₃ (mean \pm s)

	Arm swing				No arm swing			
	F_{HIP}	F_{KNEE}	F_{ANK}	F_{SHLD}	F_{HIP}	F_{KNEE}	F_{ANK}	F_{SHLD}
Instantaneous								
t_{LP}	-1.5 ± 0.2^b	-1.8 ± 0.3^b	-2.0 ± 0.3^b	0.2 ± 0.3	-1.6 ± 0.2^b	-1.9 ± 0.3^b	-2.0 ± 0.3^b	0.2 ± 0.0
t_1	-1.5 ± 0.2^b	-1.8 ± 0.2	-1.9 ± 0.2	0.8 ± 0.2^a	-1.4 ± 0.1^b	-1.8 ± 0.1	-1.9 ± 0.2	0.3 ± 0.1^a
t_2	-1.6 ± 0.1^a	-2.1 ± 0.2^a	-2.2 ± 0.2^a	0.1 ± 0.2^a	-1.3 ± 0.1^a	-1.8 ± 0.1^a	-1.9 ± 0.1^a	0.2 ± 0.0^a
t_{PV}	-0.5 ± 0.2^b	-0.8 ± 0.2	-1.1 ± 0.2	-0.2 ± 0.1^a	-0.6 ± 0.2^b	-0.9 ± 0.2	-1.2 ± 0.2	0.0 ± 0.0^a
Average								
Period C ₁	-1.5 ± 0.2^b	-1.8 ± 0.2	-1.9 ± 0.2	0.5 ± 0.2^a	-1.6 ± 0.1^b	-1.8 ± 0.2	-2.0 ± 0.2	0.3 ± 0.0^a
Period C ₂	-1.6 ± 0.1^a	-1.9 ± 0.2^a	-2.1 ± 0.2^a	0.5 ± 0.2^a	-1.4 ± 0.1^a	-1.7 ± 0.2^a	-1.8 ± 0.2^a	0.3 ± 0.0^a
Period C ₃	-1.3 ± 0.1^a	-1.8 ± 0.1^a	-2.0 ± 0.1^a	-0.1 ± 0.1^a	-1.2 ± 0.1^a	-1.6 ± 0.1^a	-1.8 ± 0.1^a	0.1 ± 0.0^a

^a Experiment-wide $P \leq 0.05$ (per comparison $P \leq 0.0005$). ^b Per comparison $P \leq 0.05$.

propulsive phase of the jump, they may selectively inactivate the hamstring muscles. The inactivation of the hamstrings coupled with the rapid concentric conditions at the hip would result in a rapid decline in hip extensor torque observed during periods C₁ and C₂ in the no-arm-swing jumps. Simultaneously, the decrease in the flexion torque at the knee associated with the hamstring activity and the increasing moment arm of the quadriceps may offset reductions in torque owing to the concentric conditions experienced by the quadriceps, and enable the knee extension torque to remain roughly constant in the no-arm-swing jumps during periods C₁ and C₂.

The above interpretation is substantiated by the findings of Gregoire *et al.* (1984) and Bobbert and van Ingen Schenau (1988), who reported electromyographic activity for the gluteus maximus, semitendinosus, biceps femoris, rectus femoris and vastus medialis throughout the propulsive phase of no-arm-swing style jumps. Gregoire *et al.* (1984) and Bobbert and van Ingen Schenau (1988) found that the electromyographic activity of the hamstrings decreased after the initial 33% of the propulsive period and speculated that the action of the hamstrings muscles was to exert a restraining influence on knee extension.

In the jumps with an arm swing, the gluteus maximus, hamstrings and quadriceps are also active at t_1 . As in the jumps without an arm swing, the arm-swing jumpers also wish to produce large knee extensor torques during the propulsive phase to continue the upward acceleration of the body during the jump. However, as the arm-swing jumpers deactivate the hamstrings, they are simultaneously placing the hip joint in slower concentric conditions by using the arm swing to decrease the rate of hip extension. Deactivation of the hamstrings coupled

with the slowing concentric conditions at the hip may result in the modest decline in hip extensor torque observed during periods C₁ and C₂ in the arm-swing jumps. Simultaneously, the elimination or reduction of the flexion torque at the knee associated with the hamstrings activity, the increasing moment arm of the quadriceps and the possible recruitment of high-threshold, fast-twitch, fatigable motor units offset the concentric conditions experienced by the quadriceps and enable the knee extension torque to increase in magnitude by approximately 28.4% in the arm-swing jumps during periods C₁ and C₂.

As a result of the arm swing and the larger hip and knee extensor torques in the arm-swing versus no-arm-swing jumps, larger downward vertical forces were applied to the thigh, shank, foot and ground by its adjacent respective proximal segment (see F_{HIP} , F_{KNEE} and F_{ANK} in Table 6 and F_z in Table 2). As a result, the vertical acceleration of the head and trunk ($a_{z\text{HT}}$) and body ($a_{z\text{G}}$) continued to increase in the arm-swing jumps during period C₂. The larger vertical accelerations for the centre of mass of the body in the arm-swing versus no-arm-swing jumps resulted in a larger change in the vertical velocity of the centre of mass of the body ($v_{z\text{G}}$) during period C₂ (arm swing: $1.13 \text{ m} \cdot \text{s}^{-1}$; no arm swing: $0.96 \text{ m} \cdot \text{s}^{-1}$) and accounted for the larger value of this variable at t_2 (Table 2).

Period C₃

During period C₃ in the arm-swing jumps, the rates of rotation of the trunk, thigh and hip increased and resulted in significantly larger values for the angular velocity of the hip (ω_{HIP}) and thigh (ω_{TH}) at the instant of maximum positive vertical velocity of the centre of

mass relative to t_2 (Fig. 6 and Table 4). In the no-arm-swing jumps, the angular velocity of the hip exhibited a smaller increase during C_3 , as reductions in the rate of trunk extension offset increasing rates of clockwise thigh rotation (Fig. 6 and Table 4). The arm-swing jumps also had larger extension angular velocities at the knee relative to the no-arm-swing jumps during period C_3 . As the angular velocity of the shank was similar in both jump styles, the differences in knee extension angular velocity were due principally to different rates of clockwise thigh rotation in the arm-swing versus no-arm-swing jumps (Table 5 and Fig. 7).

In the arm-swing and no-arm-swing jumps, the rapid extension angular velocities at the hip and knee during period C_3 were associated with large decreases in the extension torques at the hip and knee (Fig. 8). Between t_2 and the instant of maximum vertical velocity of the centre of mass of the body in both types of jump, the hip extensor torques declined by 92% and 87% respectively, and the knee extensor torques declined by 72% and 58% respectively (Tables 4 and 5). The decreases in the extensor torques at the hip and knee were primarily a result of the rapid concentric actions of the muscles at this time. Before take-off in both jump styles, it is necessary for the athlete to decrease the knee extensor torque to prevent the knee from being in a hyper-extended and possible injurious position. A decline in the hip extensor torque before take-off may also be required to position the trunk and thigh in near vertical orientations at take-off (Table 2). Thus, the athletes may have volitionally deactivated the hip and knee extensor musculature before the instant of maximum positive vertical velocity to avoid injury and maximize the height of the centre of mass of the body at take-off.

The greater magnitudes of extensor torque in the arm-swing jumps both at and immediately after t_2 were responsible for the larger average torque values at the hip and knee in the arm-swing versus no-arm-swing jumps during period C_3 (Tables 4 and 5). In turn, the larger torques at the hip and knee resulted in larger average downward vertical forces applied at the joints of the lower extremity (Table 6) and on the ground (Table 2) during period C_3 in the arm-swing jumps. During period C_3 , the vertical velocity at the centre of mass (v_{zG}) increased by $0.73 \text{ m} \cdot \text{s}^{-1}$ in the arm-swing jumps and by $0.63 \text{ m} \cdot \text{s}^{-1}$ in the no-arm-swing jumps (Table 2) and this velocity was $0.27 \text{ m} \cdot \text{s}^{-1}$ greater at the instant of maximum positive vertical velocity of the centre of mass of the body in the jumps with an arm swing.

Period D

Between the instant of maximum positive vertical velocity of the centre of mass and take-off, the torques at the hip and knee continued their rapid decline and had

small flexion values by the instant of take-off (Fig. 8). The magnitudes of the vertical forces applied to the ground by the athletes during period D were less than their body weight and the vertical acceleration of the centre of mass (a_{zG}) was negative for both the arm-swing and no-arm-swing jumps (Fig. 4). Consequently, the vertical velocity of the centre of mass (v_{zG}) decreased by approximately $0.2 \text{ m} \cdot \text{s}^{-1}$ during period D for both styles of jumps. At take-off, the vertical velocity was $2.75 \text{ m} \cdot \text{s}^{-1}$ for the arm-swing jumps and $2.44 \text{ m} \cdot \text{s}^{-1}$ for the no-arm-swing jumps. Additionally, the trunk was in a more upright position and the hips and knees were in positions of increased extension at take-off in the arm-swing versus no-arm-swing jumps (Table 3 and sequences at the top of Figs 4 and 5).

Summary

The findings of this study indicate that, during counter-movement vertical jumps, the arm swing augments the ability of the hip and knee musculature to create extensor torques during the propulsive period of the jump. By slowing the rate of counterclockwise trunk rotation as the propulsive phase of the jump is initiated, the arm swing placed the hip extensor muscles in physiological conditions that favoured the generation of large muscular tensions and torques. The arm swing also allowed the athletes to increase the extensor torque at the knee by 28% between the instant of minimum vertical displacement of the centre of mass and t_2 and when the knee extensor muscles were in concentric conditions. The mechanical, neural or physiological factors responsible for the increase in knee extensor torque between these two instants is unclear but may be due to some or all of the following factors: an increasing moment arm for the quadriceps muscles during period C_2 ; the effects of two-joint hip and knee muscles; different physiological conditions experienced by the knee muscles; altered levels of muscle activation; and different recruitment strategies for the hip and knee extensor muscles.

Acknowledgements

The authors are indebted to M. Dunphy, N. Mathies and the 1994–95 men's and women's Pepperdine University volleyball teams for their time and patience. We also acknowledge the contributions of T. Stewart, P. Mandella, M. Cox, K. Millikan, M. Davis, M. Anderson and K. Jonasson to the data collection and reduction. Lastly, we thank D.M. Kocaja for his insights regarding the neurophysiological aspects of the manuscript and M. LeBlanc for her review of the completed manuscript. The subroutines necessary to draw the jumpers in Figs 4, 5 and 10 were adapted from subroutines provided by Jes s Dapena, Department of Kinesiology, Indiana University, Bloomington, IN 47405, USA.

References

- Anderson, F.C. and Pandy, M.G. (1993). Storage and utilization of elastic strain energy during jumping. *Journal of Biomechanics*, **26**, 1413–1427.
- Andrews, J.G. (1974). Biomechanical analysis of human motion. In *Kinesiology IV*, pp. 32–42. Washington, DC: AAHPERD.
- Andrews, J.G. (1982). On the relationship between resultant joint torques and muscular activity. *Medicine and Science in Sports and Exercise*, **14**, 361–367.
- Asmussen, E. and Bonde-Peterson, F. (1974). Storage of elastic energy in skeletal muscles in man. *Acta Physiologica Scandinavica*, **91**, 385–392.
- Bobbert, M.F. and van Ingen Schenau, G.J. (1988). Coordination in vertical jumping. *Journal of Biomechanics*, **21**, 249–262.
- Cavagna, G.A., Dusman, B. and Margaria, R. (1968). Positive work done by the previously stretched muscle. *Journal of Applied Physiology*, **24**, 21–32.
- Chandler, R.F., Clauser, C.E., McConville, J.T., Reynolds, H.M. and Young, J.M. (1975). Investigation of the inertial properties of the human body. *AMRL Technical Report 74-137*. Dayton, OH: Wright Patterson Air Force Base.
- Clauser, C.E., McConville, J.T. and Young, J.W. (1969). Weight, volume and centre of mass of segments of the human body. *AMRL Technical Report 69-70*. Dayton, OH: Wright Patterson Air Force Base.
- Dapena, J. (1978). A method to determine the angular momentum of a human body about three orthogonal axes passing through its centre of gravity. *Journal of Biomechanics*, **11**, 251–256.
- Enoka, R.M. (1988). *Neuromechanical Basis of Kinesiology*. Champaign, IL: Human Kinetics.
- Feltner, M.E. and Dapena, J. (1986). Dynamics of the shoulder and elbow joints of the throwing arm during a baseball pitch. *International Journal of Sport Biomechanics*, **2**, 235–259.
- Gregoire, L., Veeger, H.E., Huijing, P.A. and van Ingen Schenau, G.J. (1984). Role of mono- and biarticular muscles in explosive movements. *International Journal of Sports Medicine*, **5**, 301–305.
- Harman, E.A., Rosenstein, M.T., Frykman, P.N. and Rosenstein, R.M. (1990). The effects of arms and countermovement on vertical jumping. *Medicine and Science in Sports and Exercise*, **22**, 825–833.
- Hay, J.G. and Reid, J.G. (1988). *Anatomy, Mechanics and Human Motion*. Englewood Cliffs, NJ: Prentice-Hall.
- Henneman, E. (1979). Functional organization of motor-neuron pools: The size principle. In *Integration in the Nervous System* (edited by H. Asanuma and V.J. Wilson), pp. 13–25. Tokyo: Igaku-Shoin.
- Herzog, W., Hasler, E. and Abrahamse, S.K. (1991). A comparison of knee extensor strength curves obtained theoretically and experimentally. *Medicine and Science in Sports and Exercise*, **23**, 108–114.
- Hill, A.V. (1938). The heat of shortening and the dynamic constants of muscle. *Proceedings of the Royal Society of London, B*, **126**, 136–195.
- Hinrichs, R.N. (1985). Regression equations to predict segmental moments of inertia from anthropometric measurements: An extension of the data. *Journal of Biomechanics*, **18**, 621–624.
- Hinrichs, R.N. (1990). Adjustments to the segment centre of mass proportions of Clauser *et al.* (1969). *Journal of Biomechanics*, **23**, 949–951.
- Jensen, R.C., Warren, B., Laursen, C. and Morrissey, M.C. (1991). Static pre-load effect and knee extensor isokinetic concentric and eccentric performance. *Medicine and Science in Sports and Exercise*, **23**, 10–14.
- Keppel, G. (1982). *Design and Analysis*. Englewood Cliffs, NJ: Prentice-Hall.
- Khalid, W., Amin, M. and Bober, T. (1989). The influence of upper extremities movement on take-off in vertical jump. In *Biomechanics in Sports V* (edited by L. Tsarouchas, J. Terauds, B. Gowitzke and L. Holt), pp. 375–379. Athens: Hellenic Sports Research Institute.
- Komi, P.V. and Bosco, C. (1978). Utilization of stored elastic energy in leg extensor muscles by men and women. *Medicine and Science in Sports and Exercise*, **10**, 261–265.
- Luhtanen, P. and Komi, P.V. (1978). Segmental contribution to forces in vertical jump. *European Journal of Applied Physiology*, **38**, 181–188.
- Miller, D.I. (1976). A biomechanical analysis of the contribution of the trunk to standing vertical jump takeoffs. In *Physical Education, Sport and the Sciences* (edited by J. Broekhoff), pp. 355–374. Eugene, OR: Microform Publications.
- Oddson, L. (1989). What factors determine vertical jumping height? In *Biomechanics in Sports V* (edited by L. Tsarouchas, J. Terauds, B. Gowitzke and L. Holt), pp. 393–401. Athens: Hellenic Sports Research Institute.
- Payne, A.H., Slater, W.J. and Telford, T. (1968). The use of a force platform in the study of athletic activities. *Ergonomics*, **11**, 123–143.
- Perrine, J.J. and Edgerton, V.R. (1978). Muscle force–velocity and power–velocity relationships under isokinetic loading. *Medicine and Science in Sports*, **10**, 159–166.
- Shetty, A.B. and Etnyre, B.R. (1989). Contribution of arm movement to the force components of a maximum vertical jump. *Journal of Orthopaedic and Sports Physical Therapy*, **11**, 198–201.
- Smidt, G.L. (1973). Biomechanical analysis of knee flexion and extension. *Journal of Biomechanics*, **6**, 79–92.
- Spoor, C.W. and van Leeuwen, J.L. (1992). Knee muscle moment arms from MRI and tendon travel. *Journal of Biomechanics*, **25**, 201–206.
- Vaughan, C.L. (1980). An optimization approach to closed loop problems in biomechanics. Unpublished doctoral dissertation, University of Iowa, Iowa City, IA.
- Wood, G.A. and Jennings, L.S. (1979). On the use of spline functions for data smoothing. *Journal of Biomechanics*, **12**, 477–479.
- Zajac, F.E. (1993). Muscle coordination of movement: A perspective. *Journal of Biomechanics*, **26**, 109–124.